

## 4D Study of Left Heart Anomalies

**Giuseppe Rizzo and Domenico Arduini**

*Department of Obstetrics and Gynecology, Università Roma "Tor Vergata" Rome Italy*

**Abstract:** In this chapter, the 2D, color Doppler and four dimensional (4D) features of major right heart abnormalities are described. In particular, the echocardiographic views on which the various lesions are present are reported. The diagnostic role of 4D echocardiography in allowing a spatial demonstration of the defects with the possibility of getting new views into the heart is outlined. Videos of major diagnostic features are also provided, to facilitate the understanding of the text.

**Key Words:** 4D Sonography, Fetal Echocardiography, Right Heart Anomalies, Prenatal Diagnosis.

### INTRODUCTION

This chapter will cover the most significant anomalies of the left side of the heart that can be observed prenatally. For each condition after a brief anatomical description, the criteria of echocardiographic diagnosis will be provided. In particular we will focus on the four dimensional (4D) acquisition and postprocessing modalities in fetal hearts with right side anomalies, demonstrating their use through case examples.

### HYPOPLASTIC LEFT HEART SYNDROME

The term Hypoplastic Left Heart Syndrome (HLHS) includes a spectrum of cardiac anomalies characterized by a marked underdevelopment of left ventricle and ascending aorta. This results in a situation where the left side of the heart is completely unable to support the circulation. Its incidence is between 0.1-0.25/1000 newborns and represents about the 10% of the congenital heart disease (CHD) [1,2]. In prenatal diagnosis series the incidence is usually reported higher 12-18% of all CHD and this is due to intrauterine mortality rate.

The "classical" form is characterized by an atresic mitral valve, an atresic aortic valve, an extremely small left ventricle with no inflow from the left atrium (Fig. 1 [video 1](#)).

There is a "minor" form where the mitral valve is small but patent and the left ventricular chamber may be recognized. Other variants of HLHS include critical aortic stenosis, the Shone complex (mitral valve anomaly, aortic coarctation and subaortic stenosis), unbalanced atrioventricular septal defects all associated with severe hypoplasia of the left ventricle and aorta.

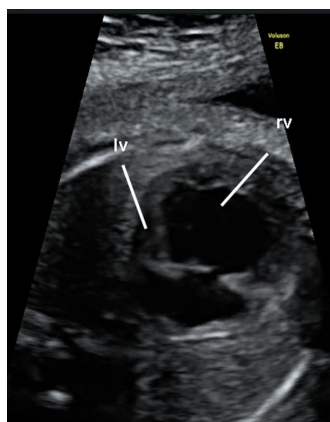


**Figure 1:** ([video 1](#)) The four chamber view of a fetus with the classical form of HLHS. The cavity of the left ventricle is difficult to identify.

\*Address Correspondence to **Giuseppe Rizzo:** Department of Obstetrics and Gynecology, Università Roma Tor Vergata Ospedale Fatebenefratelli Isola Tiberina 00186 Rome Italy; Email: giuseppe.rizzo@uniroma2.it

Color flow mapping allows to confirm the absence of filling of the left ventricle and the shunt from left to right at the level of foramen ovalis (Fig. 2, [video 2](#))

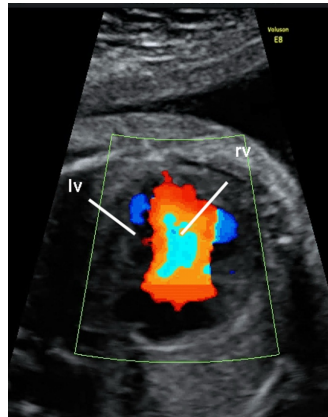


**Figure 2:** ([video 2](#)) Same fetus of Fig. 1. Color flow mapping allows to demonstrate the absence of flow through the mitral valve.

A general characteristic in all the variants of HLHS is that the right ventricle forms the apex of the heart (Fig. 3 [video 3](#))

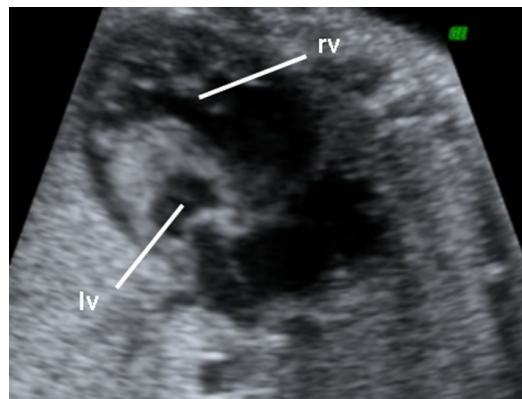


**Figure 3:** ([video 3](#)) Four chamber view in a fetus with HLHS, the left ventricle cavity is small, the walls hyperechogenic. At the apex of the heart the right ventricle (rv) is present

The ascending aorta is hypoplastic and no forward flow is detectable. Color flow mapping allows from the 3 vessel view of the fetal heart to confirm the diagnosis by showing a retrograde flow from the ductus to the aorta (Fig. 4 [video 4](#))

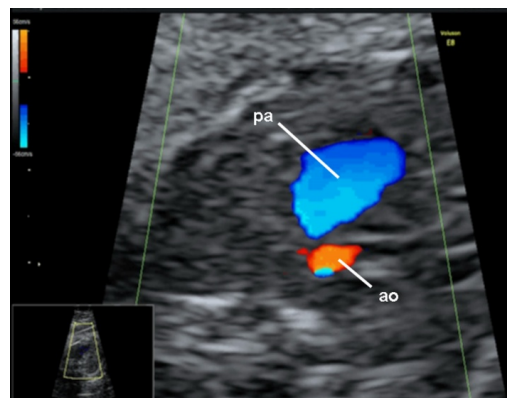


**Figure 4:** ([video 4](#)) 3 vessel view of the fetal heart in a fetus with HLHS. Normal flow direction (blue) in the pulmonary artery (PA), while there is a reverse flow (red) in the aortic trunk (ao).

The HLHS is associated with aneuploidies in about 2% of cases, particularly 45X, but also trisomy 13 and 18. Extracardiac anomalies may be present in up to 18% of cases.

The recent introduction of 4D ultrasonography to clinical practice provided an important advance in imaging technology. With a 4D acquisition of the fetal heart from the 4 chamber view it is possible to obtain few additional informations on the cardiac anatomy in HLHS. The advantages are

a) to render cardiac volume and show in more direct view the severity of the reduction of the left ventricle (Fig. 5 [video 5](#))



**Figure 5:** ([video 5](#)). Rendering of HLHS (rv right ventricle)

b) to confirm the absent inflow in the left ventricle by using the rendering function with color superimposed (Fig. 6 [video 6](#))

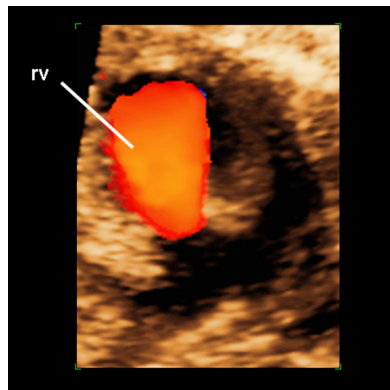


**Figure 6:** ([video 6](#)). Same fetus of Fig. 5 showing no left ventricular filling (rv right ventricle)

c) to evaluate the relative size and position of both ventricles by using render with inversion mode (Fig. 7 [video 7](#)).

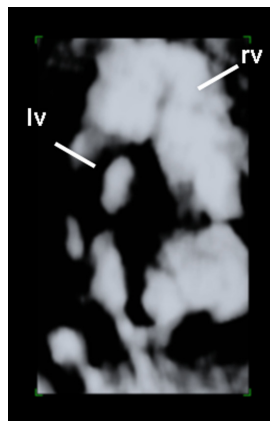


**Figure 7:** ([video 7](#)) Same fetus of Fig. 3 note the small size of the left ventricle (lv) and the right ventricle (rv) forming the apex of the heart.

## AORTIC STENOSIS

Aortic stenosis is an obstruction to the left ventricle outflow tract and the site of obstruction may be subvalvular, valvular or supra-ventricular. The incidence is of 2-3% of all CHD [1,2].

The appearance of the fetal heart will depend on the severity of the obstruction. If aortic stenosis is moderate the left ventricle usually is normal in size, or slightly reduced with a variable degree of hypertrophy of the walls (Fig. 8 [video 8](#))

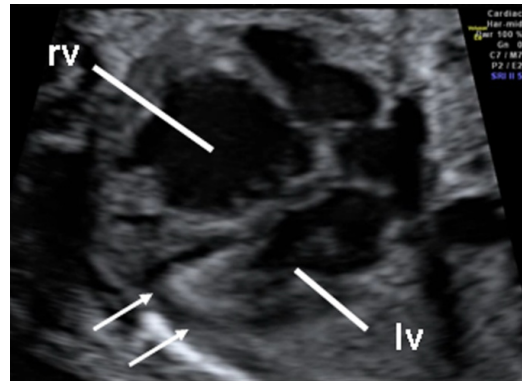


**Figure 8:** ([video 8](#)) The 4 chamber view of a fetus with moderate aortic stenosis. The left ventricle (lv) is smaller than the right ventricle (rv). The LV is hyperechogenic (arrows)

The aortic leaflets are abnormal and usually always present during all cardiac cycle (Fig. 9 [video 9](#))

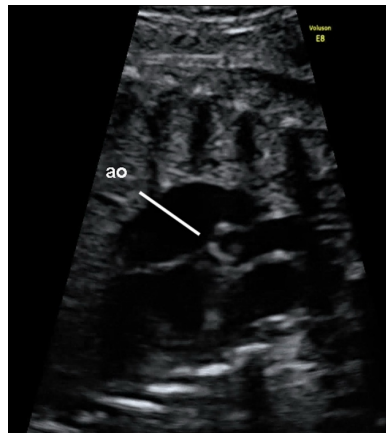


**Figure 9:** ([video 9](#)) Long axis view of the left ventricle showing a thickened aortic valve (ao)

Color flow mapping shows turbulence and increased velocities at the level of aortic valve (Fig. 10 [video 10](#))

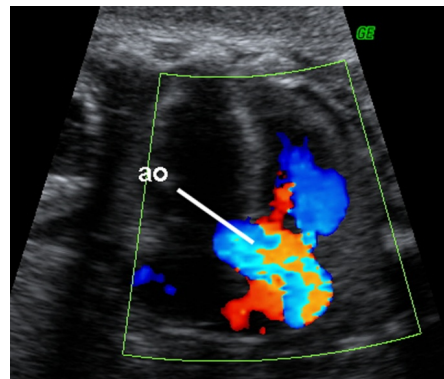


**Figure 10:** ([video 10](#)) Color flow mapping showing increased velocity at the level of ascending aorta.

that can be quantified by using spectral Doppler (Figure 11).

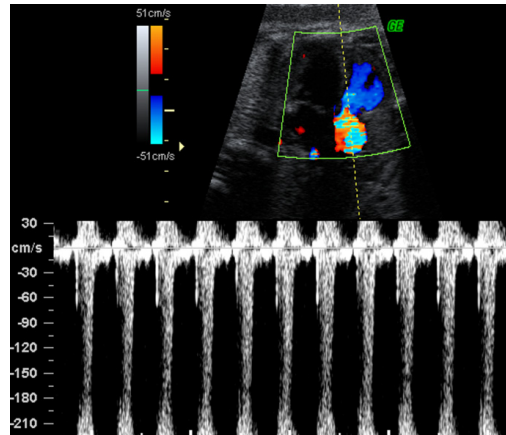


**Figure 11:** The Doppler sample volume is positioned in the ascending aorta just beyond the aortic leaflets and the velocity measured are over 210 cm/sec

Mitral regurgitation is also common due to the high pressure present in the left ventricle (Fig. 12 [video 11](#)).

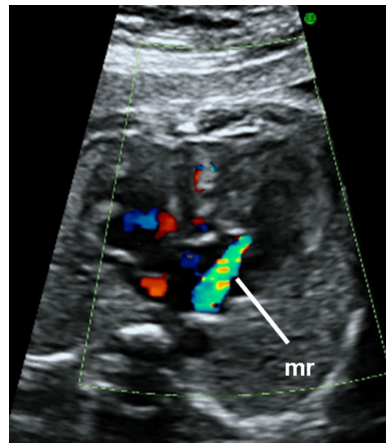


**Figure 12:** ([video 11](#)) Four chamber view of a fetus with aortic stenosis. The left atrium and left ventricles are dilated and an evident mitral regurgitation (mr) is present.

When aortic stenosis is critical the left ventricle is dilated and with poor contractility and increased echogenicity suggesting the presence of fibroelastosis. (Fig. 13 [video 12](#)).

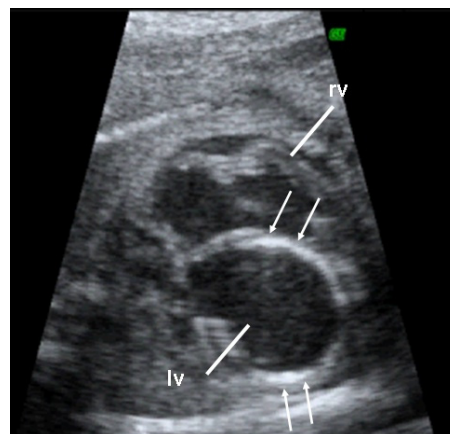


**Figure 13:** ([video 12](#)) Example of critical aortic stenosis. The left ventricle (LV) is increased in size, has poor contractility and its walls have an increased echogenicity (arrows) suggestive of fibroelastosis.

The shape of the ventricle is globular and there is difficult to document flow in the ventricle due to the poor contractility (Fig. 14 [video 13](#)).

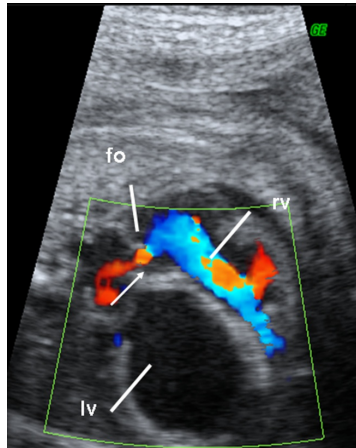


**Figure 14:** ([video 13](#)): Color flow mapping of the same fetus of Fig. 12. Note the absent filling of the left ventricle (LV) and the unidirectional flow (arrow) from the left atrium through the foramen ovale (fo) to the right ventricle

Intracardiac associated anomalies include mitral valve stenosis, ventricular septal defects (Fig. 15 [video 14](#)), restrictive foramen ovale and aortic coarctation. The Shone's Syndrome is a complex left heart disease that include mitral stenosis, aortic stenosis (usually subaortic) and coarctation.

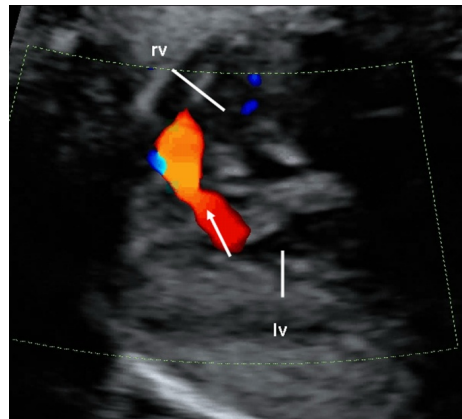


**Figure 15:** ([video 14](#)) Same fetus of figures 8 of 9. Color flow mapping allow the demonstration of a muscular ventricular septal defect. The flow is unidirectional (arrow) from the left ventricle (LV) to the right ventricle (rv) and not bidirectional as usual due to the higher pressure present in the lv for the presence of the aortic stenosis.

Extracardiac anomalies are unusual but aortic stenosis can be associated with Turner syndrome and William's syndrome (supravalvular aortic stenosis).

Aortic stenosis may be a progressive disease that from mild forms may evolve in critical stenosis with fibroelastosis or hypoplastic left heart syndrome [4]. Intrauterine treatment with balloon valvuloplasty has been suggested in the more severe form in the extent to prevent this deterioration but its role remains to be established [5, 6]

4D ultrasound provides the following advantages:

a) rendering ventricular cavity and provide indirect informations on the proportion of the two ventricles and their contractility, This informations can be obtained both using direct rendering of the fetal heart (Fig. 16, [video 15](#)) or in combination with color Doppler informations (Fig. 17 [video 16](#))

b) evaluating ventricular volume, geometry and stroke volume This is usually performed by manual methods of calculations by using software such as Organ Computer-aided AnaLysis (VOCAL) [7, 8] (see also chapter 16). (Fig. 18).

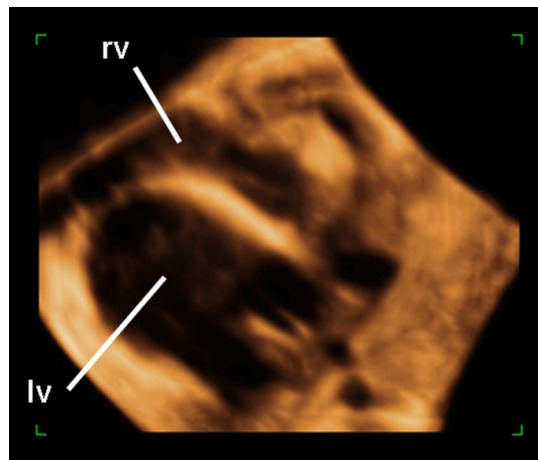


**Figure 16:** ([video 15](#)): Rendering of the four chamber view of a fetus with critical aortic stenosis and fibroelastosis. Note the enlarged left ventricle (lv) and its reduced motility. The right ventricle (rv) forms the apex.

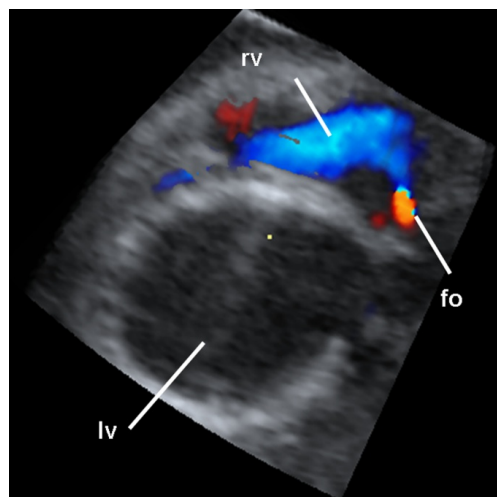


**Figure 17:** ([video 16](#)) Same fetus of Fig. 16. with rendering and color Doppler, Note the absent filling of the left ventricle (lv) and the unidirectional flow across the foramen ovalis (fo) from the left heart to the right ventricle (rv).

The manual method has the disadvantage of the relatively long time of analysis and operator dependency. To overcome these difficulties semiautomatic software for volume calculation [9] has been developed (sono-Automatic Volume Count (sonoAVC)) and these software of analysis allow reliable measurements in short time interval compatible with clinical practice [10] (Fig. 19).

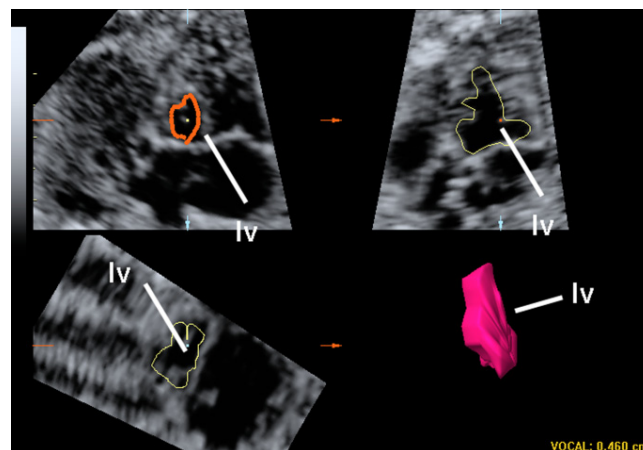


**Figure 18:** Evaluation of left ventricle (LV) with VOCAL software in a fetus with aortic stenosis.



**Figure 19:** Evaluation of left ventricle (LV) with sonoAVC software in the same fetus of Fig. 17

The evaluation of ventricular volume allows longitudinal evaluation of cardiac growth that may be useful in predicting the evolution of the disease in particular when compared to the growth of the right ventricle (Fig. 20 [video 17](#))

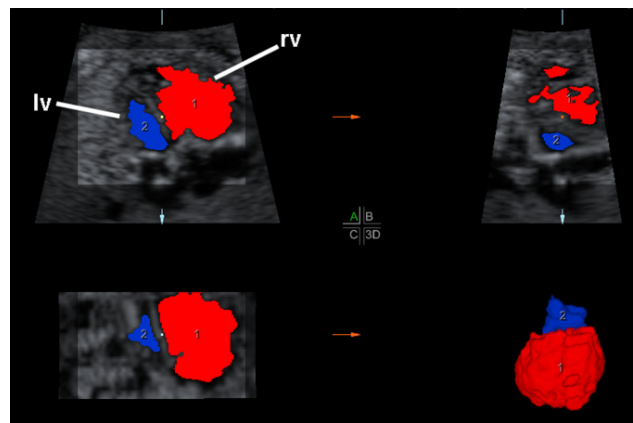


**Figure 20:** ([video 17](#)) Simultaneous assessment of left (lv blue) and right ventricle (rv red) volume by sono AVC

c) improving the diagnosis of associated intracardiac anomalies such as ventricular septal defects that can be overlooked by conventional echocardiography. In particular the application of Tomographic Ultrasound Imaging (TUI) in cardiac volumes acquired with color Doppler allows to obtain a complete view of the septum allowing an easy identification of small defects that can be difficult to evidence with 2D echocardiography [11] (Fig. 20, [video 18](#)).

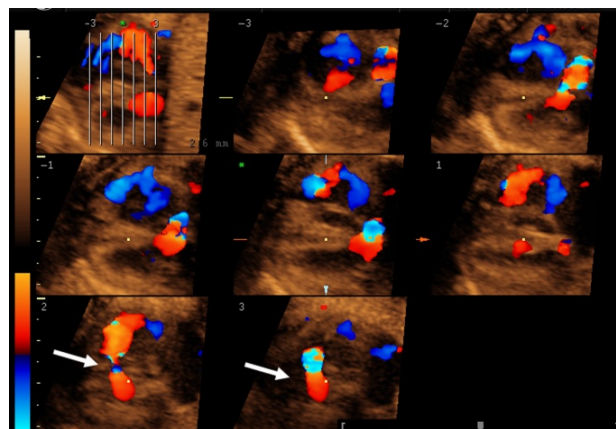


**Figure 21:** ([video 18](#)) Visualization of a muscular septal defect (arrows) with TUI technique in a cardiac volume acquired with color Doppler of a fetus with aortic stenosis.

Further evolution of this technique is the “omniview” function that allows the simultaneous view of the ventricular defect in different planes allowing a better identification and assessment of the amount and direction of the shunt between the two ventricles (Fig. 22, [video 19](#)).

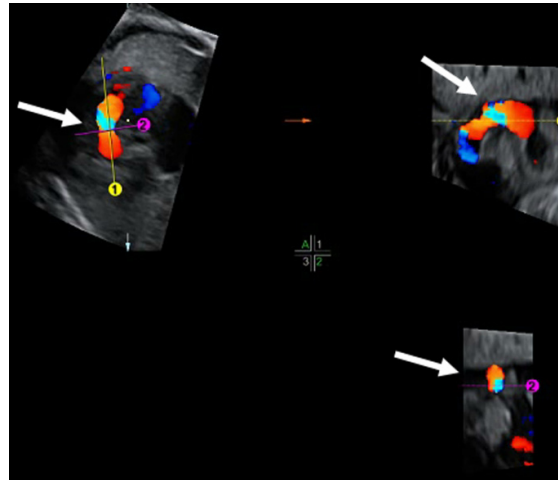


**Figure 22:** ([video 19](#)) Use of the omniview function in the same fetus of Fig. 20. The ventricular septal defect is visualized in two perpendicular planes (yellow and violet lines) allowing to confirm the unidirectional blood direction from the left ventricle to the right.

## AORTIC ARCH ANOMALIES

Aortic arch anomalies consist of several defects with different embryological etiology and the more frequent are aortic coarctation, interrupted aortic arch and right aortic arch.

### Coarctation of Aorta

Coarctation of aorta is characterized by a narrowing of the distal aortic arch (isthmus) and occurs in about 0.2-0.6% of newborns [1, 2]. Prenatal diagnosis is challenging for the difficulties of studying aortic isthmus due to the presence of the patent ductus arteriosus.

In severe case the diagnosis is suspected by the detection of a disproportion of ventricular size from the 4 chamber view [12] (Fig. 23, [video 20](#)).

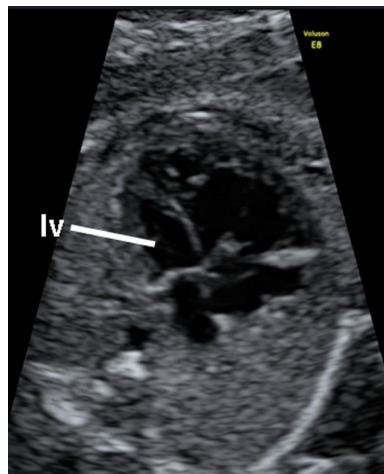


**Figure 23:** ([video 20](#)) Example of 4 chamber view in a fetus with aortic coarctation. The left ventricle (lv) is smaller than the right ventricle.

Discrepancy in the relative size of aorta and pulmonary artery [13] has been also suggested to improve the diagnosis of aortic coarctation

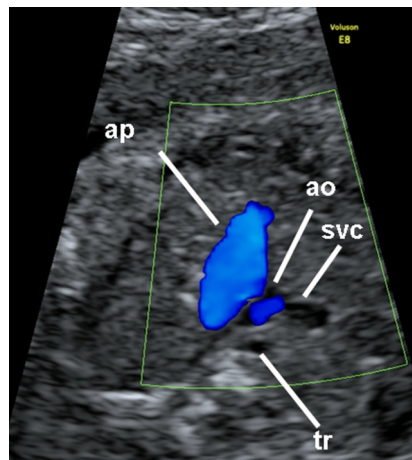


**Figure 24:** ([video 21](#)) 3 vessel and trachea (tr) view in a case of coarctation of aorta. Aorta (ao) is hypoplastic relative to pulmonary artery (pa) and superior vena cava (svc).

Simultaneous visualization of both great vessels can be obtained by the 3 vessel view (Fig. 24, [video 21](#)). In long axis view is also possible to perform comparison between aortic and ductal arch (Fig. 25 [video 22](#)) but this view has been reported as misleading [2] due to the difficulties in correctly visualizing both arches.

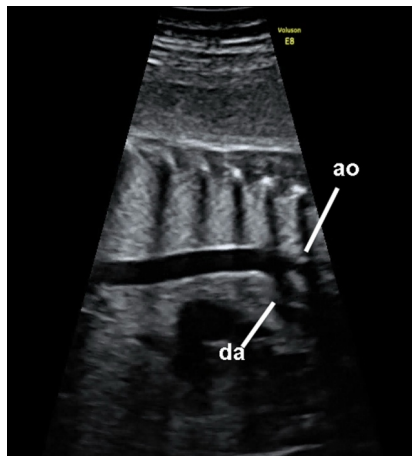


**Figure 25:** ([video 22](#)) Simultaneous visualization of aortic (ao) and ductal (da) arches in a case of coarctation of aorta. Note the reduced size of aorta when compared to ductus arteriosus.

High sensitive Doppler technique such as B flow may



**Figure 26:** ([video 23](#)) Imaging of the aortic arch by B-flow technique. Note the narrowing (arrows) of the arch when compared to descending aorta.

be used to help in delineating the narrow lumen of the aortic arch (Fig. 26 [video 23](#)).

Coarctation of the aorta may worsen with advancing gestation and subtle changes in second trimester may develop in severe forms.

In up to 60% of the cases other intracardiac anomalies are present such as atrial and ventricular defects and obstructive lesions of the left ventricle. There is also an increased incidence of extracardiac malformations and aneuploidies.

The advantages of 4D echocardiography are:

a) rendering the left ventricle cavity providing information on ventricular size and contractility (Fig. 27 [video 24](#)).



**Figure 27:** ([video 24](#)) Rendering of the four chamber view of a fetus with aortic coarctation. Note the small dimension of the left ventricle (lv) despite the normal size of aorta (ao)

b) to obtain an absolute quantification of ventricular volume and stroke volume by using VOCAL or sonoAVC software [7,8,10] as already reported for aortic stenosis.

c) easier identification of atrial and ventricular septal defects by using TUI technique [11] (see aortic stenosis)

d) reconstruction of the aortic arch by using either multiplanar display or B flow technique [14] (Fig. 28 [video 25](#)).

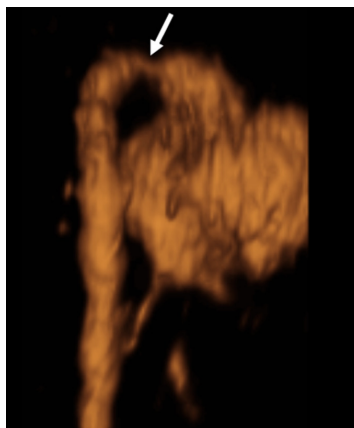


**Figure 28:** ([video 25](#)) Reconstruction of the aortic arch with rendering technique using B-flow technique. Note the narrowing (arrow) of the aortic arch

### **Interrupted Aortic Arch**

It is a rare anomaly of the aortic arch accounting for < 5% of all arch anomalies and it is divided in 3 types according to the position of the interruption:

1) type A in which the lesion is between the left subclavian artery and descending aorta and it appears as a severe form of aortic coarctation.

2) type B in which there is interruption between the left common carotid artery and the left subclavian artery

3) type C in which the interruption is between the innominate artery and the left common carotid artery and it is an extremely uncommon form

Type B is the most common disease and it is usually characterized by a disproportion of ventricular size (Fig. 29 [video 26](#)). Usually a malalignment ventricular septal defect is present.

The aorta is of reduces size with straight direction and characterized by a V shape bifurcation in the innominate artery (brachiocephalic artery) and the left common carotid artery [15] (Fig. 30 [video 27](#)).

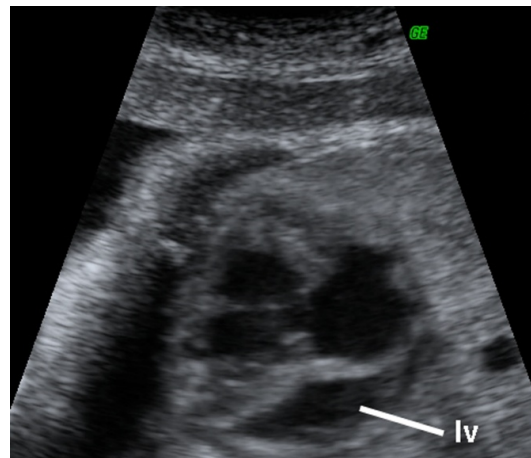


**Figure 29:** ([video 26](#)) Evident disproportion between left (lv) and right ventricle in a case with interrupted aortic arch type B.

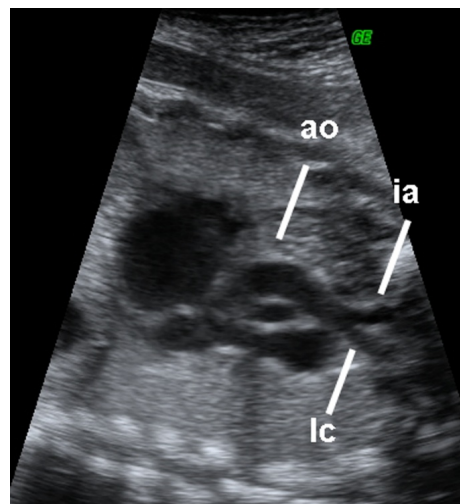


**Figure 30:** ([video 27](#)) Same fetus of figure 29. The aorta (ao) appear straight and branches in the innominate (ia) and left common carotid (lc) arteries.

Microdeletion of chromosome 22q11 is associated up to 75% of cases with type B interrupted aortic arch [16].

The advantages of 4D echoardiography are:

a) rendering the 4 chamber of the fetal heart as already show for aortic stenosis and coarctation

b) providing a topographic visualization of the malalignment ventricular septal defect and of its sizes (Fig. 31 [video 28](#))

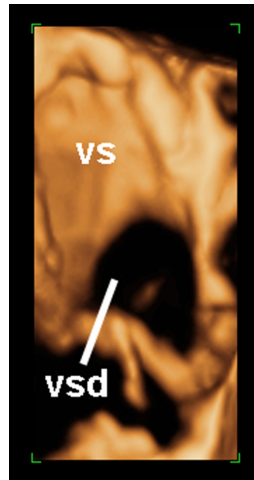


**Figure 31:** ([video 28](#)) "Enface" view of the ventricular septum (vs) in a fetus with interrupted aortic arch type B showing the malalignment ventricular septal defect (vsd).

c) reconstruction of the arch with B-flow technique (Fig. 32 [video 29](#)).

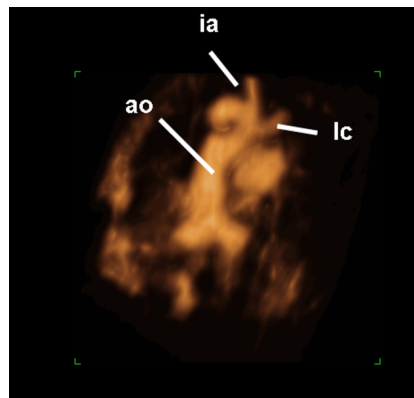


**Figure 32:** ([video 29](#)) Reconstruction of the aortic arch with rendering technique using B-flow technique in the same fetus of Fig. 30. The aorta (ao) appear straight and branches in the innominate (ia) and left common carotid (lc) arteries.

### Right Aortic Arch

It is characterized by an aortic arch that courses to the right side of the trachea and arches around the proximal part of the right main bronchus. It occurs in about 0.1% of newborns [18].

The diagnosis is done from the 3 vessel and trachea view [18] where the trachea appears between the aorta and the pulmonary artery instead of being on the right side of aorta. (Fig. 33 [video 30](#)).

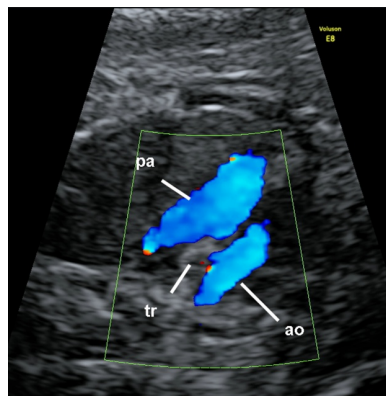


**Figure 33:** [video 30](#) 3 vessel and trachea view of a fetus with right aortic arch. The trachea (tr) is between the pulmonary artery (pa) and aorta (ao)

The right aortic arch is frequently associated with other CHD including tetralogy of Fallot, and truncus arteriosus. Less frequently is associated with tricuspid atresia, transposition of great artery and ventricular septal defects [17].

Chromosome 22q11 microdeletion are frequent and right aortic arch may be the only cardiac sign present. When an aberrant subclavian artery is present there is also an increased risk of trisomy 21 [17].

4D echocardiography provides the following advantages:

- a) allowing a multiplanar display showing the spatial relationship between the trachea and the great vessels (Fig. 34 [video 31](#))
- b) allowing an easier identification of aberrant vessel such as the right subclavian artery by using the TUI technique in volume acquired with color Doppler function (Fig. 35, [video 32](#))
- c) rendering and demonstrating the presence of vascular rings around the trachea (Fig. 36, 37, 38, [video 33](#), [video 34](#), [video 35](#))

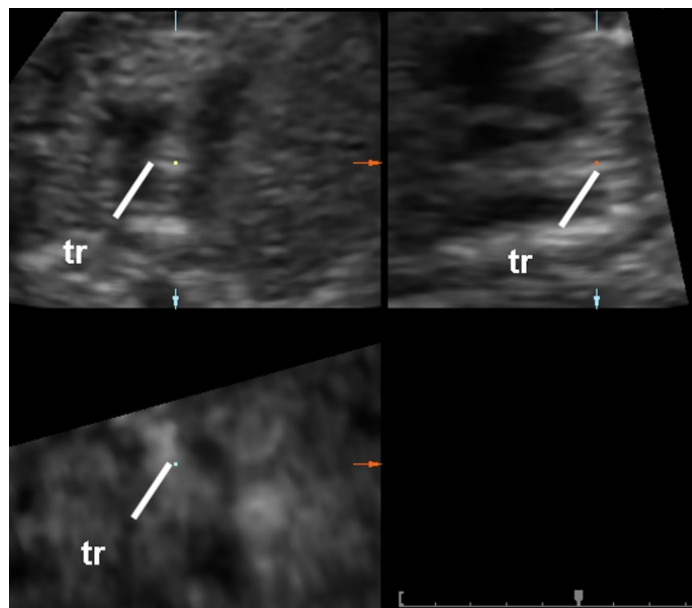


**Figure 34:** ([video 31](#)) Multiplanar display of a fetus with right aortic arch. The dot is placed on the fetal trachea (tr)

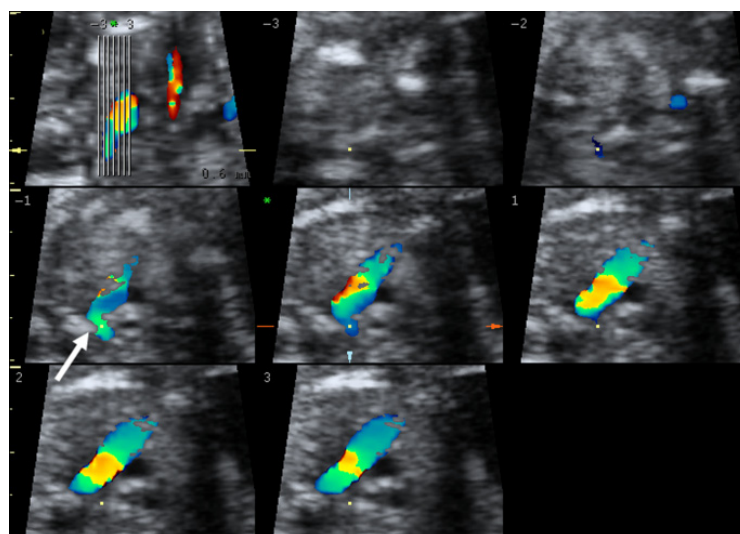


**Figure 35:** ([video 32](#)) Display of aberrant right subclavian artery (arrow) by using the TUI technique

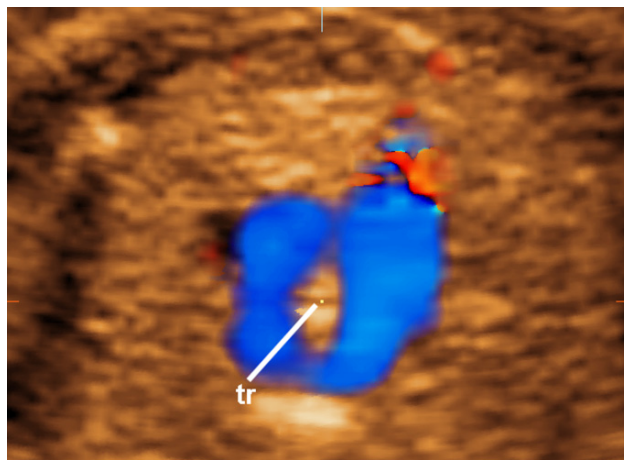


**Figure 36:** ([video 33](#)) Example of vascular ring with the vascular encirclement of the trachea (tr)

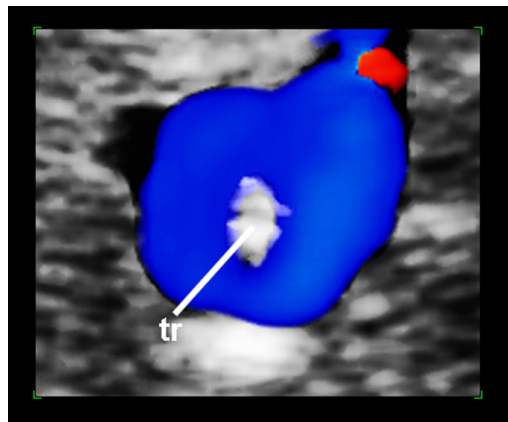


**Figure 37:** ([video 34](#)) Glass body display of the same fetus of Fig. 36

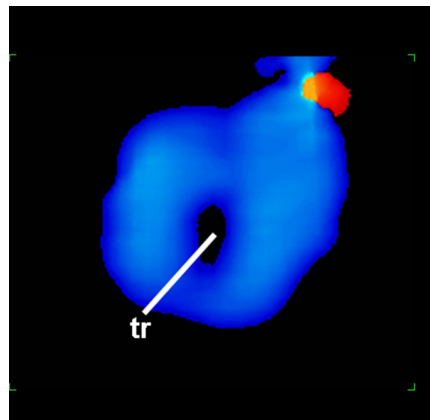


**Figure 38:** ([video 35](#)) Glass body display of the same fetus of Fig. 36

## REFERENCES

- [1] Allan L, Honberger L, Sharland G Textbook of fetal cardiology Greenwich Medical Media London, 2000.
- [2] Allan LD Left heart malformations. In Fetal cardiology. Yagel S, Silverman NH, Gembruch U 2<sup>nd</sup> Edition, pp 291-303, 2009, Informa Healthcare New York Publisher.
- [3] Simpson JM Hypoplastic left heart syndrome. *Ultrasound Obstet Gynecol* 2000, 15: 271-278.
- [4] Mäkikallio K, McElhinney DB, Levine JC, Marx GR, Colan SD, Marshall AC, Lock JE, Marcus EN, Tworetzky W. Fetal aortic valve stenosis and the evolution of hypoplastic left heart syndrome: patient selection for fetal intervention. *Circulation* 2006; 113: 1401-1405.

- [5] Kleinman CS. Fetal cardiac intervention: innovative therapy or a technique in search of an indication? *Circulation* 2006 113:1378-1381.
- [6] Gardiner HM. In-utero intervention for severe congenital heart disease. *Best Pract Res Clin Obstet Gynaecol.* 2008; 22:49-61.
- [7] Rizzo G, Capponi A, Cavicchioni O, Vendola M, Arduini D. Fetal cardiac stroke volume determination by four-dimensional ultrasound with spatio-temporal image correlation compared with two-dimensional and Doppler ultrasonography. *Prenat Diagn* 2007; 27: 1147-50.
- [8] Hamill N, Romero R, Hassa S, Lee W, Myers PA, Mitta I, Kusanovi JPC, Chaiworapongs T, Vaisbuc D, Espinoza, J, Gotsch F, Carletti A, Gonçalves LF, Lami Y Repeatability and Reproducibility of Fetal Cardiac Ventricular Volume Calculations Using Spatiotemporal Image Correlation and Virtual Organ Computer-Aided Analysis *J Ultrasound Med* 2009 28: 1301-1311.
- [9] Tutschek B, Sahn DJ. Semi-automatic segmentation of fetal cardiac cavities: progress towards an automated fetal echocardiogram. *Ultrasound Obstet Gynecol* 2008 32:176-180.
- [10] Rizzo G, Capponi A, Pietrolucci ME, Arduini D. The role of sono-Automatic Volume Count (sonoAVC) in measuring fetal cardiac ventricular volumes using four dimensional ultrasound: comparison with Virtual Organ Computer-aided AnaLysis (VOCAL) *J Ultrasound Med* 2010; 29 : 260-70.
- [11] Rizzo G, Capponi A, Vendola M, Pietrolucci ME, Arduini D. Role of tomographic ultrasound imaging with spatiotemporal image correlation for identifying fetal ventricular septal defects. *J Ultrasound Med* 2008; 27:1071-1075.
- [12] Matsui H, Mellander M, Roughton M, Jicinska H, Gardiner HM Morphological and physiological predictors of fetal aortic coarctation. *Circulation.* 2008;118: 1793-1801
- [13] Slodki M, Rychik J, Moszura T, Janiak K, Respondek-Liberska M Measurement of the great vessels in the mediastinum could help distinguish true from false-positive coarctation of the aorta in the third trimester. *J Ultrasound Med.* 2009 28: 1313-1317.
- [14] Espinoza J, Romero R, Kusanovic JP, Gotsch F, Erez O, Hassan S, Yeo L. Prenatal Diagnosis of Coarctation of the Aorta With the Multiplanar Display and B-Flow Imaging Using 4-Dimensional Sonography *J Ultrasound Med* 2009 28: 1375-1378.
- [15] Volpe P, Marasini M, Caruso G, Gentile M. Prenatal diagnosis of interruption of the aortic arch and its association with deletion of chromosome 22q11. *Ultrasound Obstet Gynecol.* 2002 20:327-31
- [16] Volpe P, Marasini M, Caruso G, Marzullo A, Buonadonna AL, Arciprete P, Di Paolo S, Volpe G, Gentile M. 22q11 deletions in fetuses with malformations of the outflow tracts or interruption of the aortic arch: impact of additional ultrasound signs. *Prenat Diagn.* 2003;23:752-7.
- [17] Yoo SJ, Bradley T, Jaeggi E Aortic arch anomalies. In *Fetal cardiology.* Yagel S, Silverman NH, Gembruch U 2<sup>nd</sup> Edition, pp 329-342, 2009, Informa Healthcare New York Publisher.
- [18] Tuo G, Volpe P, Bava GL, Bondanza S, De Robertis V, Pongiglione G, Marasini M. Prenatal diagnosis and outcome of isolated vascular rings. *Am J Cardiol.* 2009 ;103 :416-419.